EBioMedicine 48 (2019) 491–504

Contents lists available at ScienceDirect

EBioMedicine

journal homepage: www.elsevier.com/locate/ebiom

EBioMedicine
Published by THE LANCET

FoxO1-mediated inhibition of STAT1 alleviates tubulointerstitial fibrosis and tubule apoptosis in diabetic kidney disease

Fengjuan Huang[a,b], Qingzhu Wang[a], Feng Guo[a], Yanyan Zhao[a], Linlin Ji[b], Tingting An[b], Yi Song[b], Yang Liu[b], Yanyan He[b], Guijun Qin[a,*]

[a] Division of Endocrinology, Department of Internal Medicine, The First Affiliated Hospital of Zhengzhou University, Zhengzhou 450052, China
[b] Institute of Clinical Medicine, The First Affiliated Hospital of Zhengzhou University, Zhengzhou 450052, China

ARTICLE INFO

Article history:
Received 31 July 2019
Revised 27 August 2019
Accepted 3 September 2019
Available online 16 October 2019

Keywords:
FoxO1
STAT1
Apoptosis
Diabetic kidney disease
Tubulointerstitial fibrosis

ABSTRACT

Background: Tubulointerstitial fibrosis (TIF) plays an important role in the progression of diabetic kidney disease (DKD). Forkhead box O1 (FoxO1) is involved in the regulation of metabolism and cell apoptosis, but its function in renal TIF induced by DKD is less well understood.

Methods: Human kidney biopsies with DKD and normal controls were used to detect apoptosis and TIF induced by diabetes. A mouse model with kidney-specific overexpression of Pax2-3aFoxO1 was established to further investigate the functions of FoxO1 in vivo. The in vitro roles of FoxO1 were analyzed in HK-2 cells with 3aFoxO1-knockin (3aFoxO1-KI) or FoxO1-knockdown (FoxO1-KD) via CRISPR/Cas9. Western blot, immunohistochemistry, and chromatin immunoprecipitation were used to explore the underlying mechanisms.

Findings: In this study, DKD patients had increased renal TIF and apoptosis. In vivo study showed that kidney-specific overexpression of Pax2-3aFoxO1 significantly reduced the expression of p-STAT1 with resultant renal functional impairment, retarding renal TIF and apoptosis in diabetic mice. Meanwhile, We observed that FoxO1-KD in HK-2 cells aggravated the expression of p-STAT1, leading to activation of epithelial-to-mesenchymal transition (EMT) and intrinsic apoptotic pathway. Conversely, EMT and apoptosis were significantly attenuated in HK-2 cells with 3aFoxO1-KI under hyperglycemic conditions.

Interpretation: Taken together, these data suggest that the protection role of FoxO1 against renal TIF and apoptosis in DKD is likely in part to target STAT1 signaling, which may be a promising strategy for long-term treatment of DKD.

Fund : This work was supported by grants from the National Natural Science Foundation of China (grant numbers: 81570746 and 81770812).

* Corresponding author at: Division of Endocrinology, Department of Internal Medicine, The First Affiliated Hospital of Zhengzhou University, 40 Daxue Road, Zhengzhou 450052, China.
E-mail address: hyqingj@zzu.edu.cn (G. Qin).

https://doi.org/10.1016/j.ebiom.2019.09.002

Research in context

Evidence before this study

Diabetic kidney disease (DKD) affects >20% of all diabetic patients, and tubulointerstitial fibrosis (TIF) is the final common pathway for many chronic kidney diseases (CKDs), which leads to end-stage renal failure due to limited therapeutic options. Forkhead box O1 (FoxO1), a prominent member of the forkhead box family, is involved in the regulation of cell proliferation, oxidative stress, extracellular matrix accumulation and epithelial-mesenchymal transdifferentiation (EMT) in podocytes and Mesangial cells. However, the role of FoxO1 in TIF induced by diabetes has not been extensively studied.

Added value of this study

In this study, we found that STAT1 expression was highly upregulated in the kidneys from patients with DKD and diabetic mice with the deactivation of FoxO1, which is essential for cell apoptosis and renal fibrosis. Importantly, we found that 3aFoxO1 overexpression in kidney and tubular cells resulted in nuclear accumulation of FoxO1 and a reduction in cell apoptosis and EMT through binding with STAT1 promoter.

In contrast, we found that loss of FoxO1 aggravated the expression of STAT1, leading to activation of epithelial-to-mesenchymal transition (EMT) and intrinsic apoptotic pathway.

Implications of all the available evidence

This study revealed that FoxO1 overexpression protected from the development of renal tubulointerstitial fibrosis and apoptosis induced by diabetes, which strongly suggest that targeting FoxO1/STAT1 axis represents a new therapeutic approach to retard the progression of DKD and renal function decline.

1. Introduction

Diabetic kidney disease (DKD) is the major cause of end-stage renal disease (ESRD), which is associated with a high mortality rate, and its prevalence is steadily increasing globally [1] . Although albuminuria is classically regarded a consequence of diabetes-induced glomerular damage, it is increasingly recognized that the renal tubulointerstitium also plays an important role in the pathogenesis of DKD [2]. Renal tubulointerstitial fibrosis (TIF) is characterized by the deposition of extracellular matrix (ECM), including fibronectin (FN) and collagen I (Col I) [3,4] . Growing evidences demonstrate that epithelial-to-mesenchymal transition (EMT) in tubular epithelial cells (TECs) may be involved in the progression of DKD, in which TECs start to express fibroblast markers and lose their epithelial features [5], which ultimately leads to ECM remodelling and TIF in DKD. However, the molecular mechanisms underlying TIF in DKD remain incompletely understood, and potential strategies based on blood glucose and blood pressure control are insufficient to prevent disease progression [6]. Thus, it is crucial to identify a new therapeutic approach to retard the progression of TIF and renal function decline.

Forkhead box O1 (FoxO1), a prominent member of the forkhead box family and subfamily O of transcription factors encoded by the *FKHR* gene [7], is involved in the regulation of metabolism, cell proliferation, oxidative stress, and cell death [8] . Recent studies have demonstrated that high glucose (HG) induces FoxO1 phosphorylation at Thr-24, Ala-24, Ser-253 in kidney, which is associated with its nuclear export and consequently weakened transcriptional activities, leading to ECM deposition in mesangial cells [9,10] and podocytes [11].

The Janus kinase/signal transducers and activators of transcription (JAK/STAT) pathway is an essential intracellular mechanism activated by cytokines and diabetic factors that regulates cell activation, proliferation, and differentiation [12] . STAT1 is a member of the STAT family and functions as a signal messenger and transcription factor [13], which regulates the expression of gene related with cell proliferation, oxidative stress and apoptosis [14–16] . Previous studies showed that STAT1 activation (the phosphorylated form of STAT1, p-STAT1) can be implicated in both TIF and EMT in several conditions, including diabetes, in animal models [17–20] . Recent data suggest that re-expression of FoxO1 decreases the STAT1 expression in mesangial cells under HG condition [21] . Moreover, silencing *STAT1* could reverse HG-triggered podocytes injury, which might be involved in FoxO1 mediated-oxidative stress in nucleus [22] . Based on these studies, we hypothesize that FoxO1 may retard renal TIF and tubular apoptosis through STAT1 signaling pathway.

In this study, human kidney biopsies with DKD and non-diabetic biopsies from unaffected portions of the kidney tumor (normal control, NC) were used to detect renal TIF. We then evaluated the function of FoxO1 and STAT1 in vivo and in vitro experiments. Our findings suggest an important role for FoxO1 in DKD progression and provide an effective therapeutic target for renal TIF and tubular apoptosis induced by diabetes.

2. Materials and methods

2.1. Human kidney biopsies

Human kidney biopsy specimens from patients with diabetic kidney disease (DKD, $n = 5$) were obtained from the first affiliated hospital of Zhengzhou University between 2016 and 2017, and non-diabetic biopsies from unaffected portions of the kidney tumor with normal renal function were served as normal controls (NC, $n = 5$). The Ethics Committee from Zhengzhou University approved the use of patient tissue samples in this study. The morphological diagnosis of DKD was confirmed by histological examination by a renal pathologist through hematoxylin-eosin (HE), periodic acid-Schiff (PAS), picrosirius red (PSR) and Masson staining.

2.2. Kidney-specific Pax2-3aFoxO1 mice

Briefly, 3aFoxO1-coding sequences based on mouse FoxO1 sequence with three conservative serine/threonine sites mutated (Thr-24 → Ala-24, Ser-253 → Ala-253, Ser-319 → Ala-319) were ligated downstream of *Pax2* promoter, and microinjected into fertilized eggs of C57/BL6 mouse. DNA was isolated from mouse tails and identified by PCR and gene sequencing, wild-type (WT) littermates were used as normal controls.

2.3. Type 1 diabetes mouse model

Type 1 diabetes was induced as previously described [23]. Briefly, after 12 h of fasting, six-week-old WT and Pax2-3aFoxO1 male mice were given a single intraperitoneal injection of 130 mg kg^{-1} streptozotocin (STZ, Sigma, St Louis, MO, USA) freshly prepared in 0.05 M citrate buffer (pH 4.5). The induction of diabetes was confirmed as fasting blood glucose level higher than 16.7 mmol L^{-1}. The mice were kept on a 12-h/12-h light/dark cycle at 23 ± 1 °C, with 50 ± 10% relative humidity, under specific pathogen-free conditions. All animals had free access to drinking water. The mice were divided into 4 groups ($n = 5$ per group), and

sacrificed at 16 weeks post treatment. All procedures conducted in accordance with the Principles of Laboratory Animal Care, and were approved by the institutional committees of the Animal Research Committee and Animal Ethics Committee of Zhengzhou University.

2.4. Metabolic data in diabetic mice

Fasting blood glucose was measured monthly from mouse tail veins using a blood glucose meter (ACCU-CHEK Performa, Roche Diagnostics, Germany). 24-h urine collection was carried out every month using metabolic cages. 24 h urinary total protein (24 h-UTP) was measured by ELISA quantification set (Bethyl Laboratories, Texas, USA). Blood samples were collected from the heart of anesthetized mice. Blood urea nitrogen (BUN) was measured using commercial ELISA kits (Bethyl Laboratories), and creatinine in urine and plasma was determined by HPLC (Agilent HP1100 system; Hewlett Packard, Germany) as recommended. Renal function was considered with calculation of creatinine clearance (CrCl).

2.5. Histopathology and morphometric studies by light microscopy

Kidney samples were fixed in 10% buffered formalin and embedded in paraffin for histological analysis. Histology was assessed by PAS (Jiancheng Bioengineering Institute, Nanjing, China), Masson and PSR staining (Solarbio Life Sciences, Beijing, China) according to the manufacturers' protocols [24] . Tubule morphology was measured by HE staining (Labio Experimental Audio Supplies, Zhengzhou, China). Immunohistochemistry and immunofluorescence staining were performed as previously described [23]. Briefly, kidney sections of 4 μm were incubated with primary antibodies at 4 °C overnight, followed by incubation with horseradish peroxidase-conjugated or Cy3-conjugated (1:100; Songon Biotech, Shanghai, China.) anti-rabbit secondary antibody. Then, sections were stained with DAPI or hematoxylin after being developed with diaminobenzidine. Light microscope (Olympus, Tokyo, Japan) was used to evaluate sections, and quantification of staining was performed using Image J as described.

2.6. TUNEL assay

Apoptosis were detected using In Situ Cell Death Detection Kit (Roche, Germany) in the kidney of human and diabetic mice as described.

2.7. Cell culture

HK-2 cells were purchased from the Cell Bank of Type Culture Collection (Chinese Academy of Sciences, Shanghai, China) and cultured in Dulbecco's modified Eagle's medium supplemented with 10% fetal bovine serum (Gibco), 1% penicillin (100 units mL^{-1})-streptomycin (100 $\mu g\,mL^{-1}$) at 37 °C in a humidified atmosphere of 5% CO_2. HK-2 cells were grown to 80% confluence and incubated in a serum-free medium overnight, then maintained in normal glucose (NG, 5.6 mM) or high glucose (HG, 12.5 mM and 25 mM) for 48 h according to the experiment. All experiments were performed in triplicate.

2.8. Generation of 3aFoxO1-KI and FoxO1-KD HK-2 cells via CRISPR/Cas9

Briefly, 3aFoxO1 donor plasmids with three conservative serine/threonine sites mutated were assembled, then co-transfected into HK-2 cells with Human Safe Harbor Gene Knock-in kits (GeneCopoeia, USA). FoxO1-KD HK-2 cells were obtained by three different sgRNA plasmids targeting the first exon of *FoxO1*.

2.9. STAT1 siRNA transfection

HK-2 cells seeded in 6-well plates were transfected with 20 nmol L^{-1} of STAT1 siRNA using Lipofectamine 2000 (Invitrogen, Carlsbad, CA, USA), and incubated with antibiotic-free HG medium (25 mM) for 48 h for western blot and RT-PCR analysis.

2.10. Flow cytometry

Apoptosis were detected by flow cytometry (BD FACSCalibur, San Jose, CA, USA) by Annexin V-FITC Apoptosis Detection Kit (BestBio, Shanghai, China) in HK-2 cells. Briefly, HK-2 cells were washed with cold PBS, treated with 0.25% trypsin, and then labelled with Annexin V-FITC and propidium iodide, with excitation at 488 nm.

2.11. Real-time PCR

Total RNA was isolated using TRIzol reagent (Takara, Shiga, Japan) and then reverse transcribed into first-strand cDNA using an AMV First Strand cDNA Synthesis Kit (Biological Engineering, Shanghai, China). Real-time PCR was performed using SGExcel Ultra SYBR Mixture (Biological Engineering, Shanghai, China) on 7500 Fast Real-Time PCR System (Applied Biosystems, Foster City, CA, USA). Thermal cycles were as follows: 3 min at 95 °C, 40 cycles of 95 °C for 20 s, 60 °C for 30 s, and 72 °C for 25 s. The $2^{-\Delta\,Ct}$ method was used to calculate relative gene expression, using *GAPDH* as endogenous control. All reactions were run in triplicate. Primers were designed using NCBI Primer-BLAST (Supplemental Table 1).

Total RNA was isolated using TRIzol reagent (Takara, Shiga, Japan) and then reverse transcribed into first-strand cDNA using an AMV First Strand cDNA Synthesis Kit (Biological Engineering, Shanghai, China). Real-time PCR was performed using SGExcel Ultra SYBR Mixture (Biological Engineering, Shanghai, China) on 7500 Fast Real-Time PCR System (Applied Biosystems, Foster City, CA, USA). Thermal cycles were as follows: 3 min at 95 °C, 40 cycles of 95 °C for 20 s, 60 °C for 30 s, and 72 °C for 25 s. The $2^{-\Delta\,Ct}$ method was used to calculate relative gene expression, using *GAPDH* as endogenous control. All reactions were run in triplicate. Primers were designed using NCBI Primer-BLAST (Supplemental Table 1).

2.12. Western blot

Renal cortex and HK-2 cells were lysed with RIPA Lysis Buffer containing a cocktail of 1% protease and 1% phosphatase inhibitors (ComWin Biotech, Beijing, China), and then quantified using BCA assay reagent kit (Dingguo, Beijing, China). Lysates were subjected to immunoblot analysis using primary antibody: anti-ACTB (Sangon Biotech; D110001), anti-FoxO1 (Abcam; ab39670), anti-pFoxO1 (Sangon Biotech; D155054), anti-STAT1(CST; 9172), anti-pSTAT1 (Tyr701) (Cell Signaling Technology; 9167), anti-TGFβ1 (Cell Signaling Technology; 3711), anti-Collagen I antibody (Abcam; ab6308), anti-fibronectin (Proteintech, 15613-1-AP), anti-*E*-Cadherin (Cell Signaling Technology; 3195), anti-alpha-Smooth Muscle Actin (Novus; NB600). Protein bands were detected by enhanced chemiluminescence substrate (Thermo Fisher Scientific, Waltham, MA, USA). Relative protein expression was quantified using Image J.

2.13. ChIP assay

The ChIP assay was performed according to the protocol of the EZ-ChIP Kit (Millipore, Billerica, MA) [25] . Briefly, cells were chemically cross-linked with 1% formaldehyde solution for 10 min. Then, the chromatin extract was precleared and incubated with anti-STAT1 at 4 °C. The sequence containing the STAT1-binding site in

the *FoxO1* promoter region was analyzed by PCR, and the intensity was normalized to the level of input by using the same primers. IgG was used as an isotype control and input DNA was amplified for each sample in parallel runs.

2.14. Statistical analysis

Statistical analyses were performed using GraphPad Prism 6.0 (GraphPad Software Inc.). Data are presented as the mean ± SEM. Comparison of two groups in patients was performed by unpaired *t*-tests. Differences between multiple groups were evaluated with one-way analysis of variance (ANOVA) followed by Bonferroni's comparison. *P*-values <.05 were regarded statistically significant.

3. Results

3.1. Tubular FoxO1 and STAT1 expression in renal biopsies of patients with DKD

To assess the role of FoxO1 and STAT1 in tubulointerstitial fibrosis (TIF) induced by DKD, the expression of FoxO1, pFoxO1and STAT1 was detected in human kidney biopsies with DKD and normal controls (NC). Immunostaining and quantification in renal biopsies from patients with DKD showed more intense staining of p-FoxO1, p-STAT1 and STAT1 expression in the tubules but no significant change in total FoxO1 level as compared to NC groups (Fig. 1A-H). Furthermore, we observed an increase in p-FoxO1, p-STAT1 and STAT1 expression in kidney biopsies with DKD, however, there was no change in FoxO1 by western blot and RT-PCR (Fig. 1I-M). PSR and Masson staining indicated that renal TIF was prominent in kidney tissues of DKD patients in comparison to NC (Fig. 2A-B). Moreover, thickness of tubular basement membrane enhanced in patients with DKD as illustrated by HE and PAS staining (Fig. 2A-B). In addition, we found a marked increase in Col I as well as FN expression in DKD patients (Fig. 2C-I). The clinical baseline characteristics of subjects was shown in Supplemental Table 2.

To assess the role of FoxO1 and STAT1 in tubulointerstitial fibrosis (TIF) induced by DKD, the expression of FoxO1, pFoxO1and STAT1 was detected in human kidney biopsies with DKD and normal controls (NC). Immunostaining and quantification in renal biopsies from patients with DKD showed more intense staining of p-FoxO1, p-STAT1 and STAT1 expression in the tubules but no significant change in total FoxO1 level as compared to NC groups (Fig. 1A-H). Furthermore, we observed an increase in p-FoxO1, p-STAT1 and STAT1 expression in kidney biopsies with DKD, however, there was no change in FoxO1 by western blot and RT-PCR (Fig. 1I-M). PSR and Masson staining indicated that renal TIF was prominent in kidney tissues of DKD patients in comparison to NC (Fig. 2A-B). Moreover, thickness of tubular basement membrane enhanced in patients with DKD as illustrated by HE and PAS staining (Fig. 2A-B). In addition, we found a marked increase in Col I as well as FN expression in DKD patients (Fig. 2C-I). The clinical baseline characteristics of subjects was shown in Supplemental Table 2.

3.2. Apoptosis of renal proximal tubular cells (PTCs) in DKD patients

To further demonstrate the activation of intrinsic apoptotic pathway in patients with DKD, TUNEL assay was utilized. We observed a significant increase in TUNEL+ tubular cells, supporting that DKD significantly induced renal tubular epithelial cell apoptosis (Fig. 3A-B). In addition, we assessed the expression of Bax and Bcl2 by using RT-PCR and western blotting. As shown, the mRNA and protein of Bax expression was increased, whereas Bcl-2 expression decreased in the DKD patients as compared with NC group (Fig. 3C-G).

3.3. Kidney-specific Pax2-3aFoxO1 improves renal function in diabetic mice

To ascertain the mechanism by which 3aFoxO1 reduces kidney injury under diabetes conditions, we utilized the previously validated kidney-specific Pax2-3aFoxO1 (Pax2-3aFoxO1) mice on the C57BL/6 background [26] (Supplementary Fig. 1). Blood glucose (BG) was similarly elevated in both WT and Pax2-3aFoxO1 diabetic mice at 16 weeks (Supplementary Fig. 2). Blood urea nitrogen (BUN), serum creatinine (Scr), urinary creatinine (Ucr), kidney injury molecule-1 (KIM-1) and 24-h urine total protein (24 h-UTP) were all elevated in diabetic WT mice but were significantly reduced in the diabetic Pax2-3aFoxO1 mice (Supplementary Fig. 2). Meanwhile, we also observed a significant drop in creatinine clearance (CrCl) in diabetic WT mice, which was markedly abated in diabetic Pax2-3aFoxO1 mice (Supplementary Fig. 2). Collectively, these data demonstrated that enhanced Pax2-3aFoxO1 in kidney was beneficial and protected renal function in diabetic mice.

To ascertain the mechanism by which 3aFoxO1 reduces kidney injury under diabetes conditions, we utilized the previously validated kidney-specific Pax2-3aFoxO1 (Pax2-3aFoxO1) mice on the C57BL/6 background [26] (Supplementary Fig. 1). Blood glucose (BG) was similarly elevated in both WT and Pax2-3aFoxO1 diabetic mice at 16 weeks (Supplementary Fig. 2). Blood urea nitrogen (BUN), serum creatinine (Scr), urinary creatinine (Ucr), kidney injury molecule-1 (KIM-1) and 24-h urine total protein (24 h-UTP) were all elevated in diabetic WT mice but were significantly reduced in the diabetic Pax2-3aFoxO1 mice (Supplementary Fig. 2). Meanwhile, we also observed a significant drop in creatinine clearance (CrCl) in diabetic WT mice, which was markedly abated in diabetic Pax2-3aFoxO1 mice (Supplementary Fig. 2). Collectively, these data demonstrated that enhanced Pax2-3aFoxO1 in kidney was beneficial and protected renal function in diabetic mice.

3.4. Pax2-3aFoxO1 overexpression attenuates renal TIF in diabetic mice

The degree of renal TIF was detected in the kidneys of diabetic WT and Pax2-3aFoxO1 mice. HE and PAS staining revealed that diabetes increased tubulointerstitial glycogen deposition in WT diabetic mice, whereas notably attenuated in diabetic Pax2-3aFoxO1 mice (Fig. 4A-B, E). In addition, PSR and Masson staining showed a reduction in tubulointerstitial collagen expression in the diabetic Pax2-3aFoxO1 mice as compared to diabetic WT mice (Fig. 4C-D, F-G). Furthermore, immunohistochemical staining for the interstitial Col I and FN showed that the diabetes associated increase in these collagens was significantly attenuated by Pax2-3aFoxO1 overexpression (Fig. 5A-D). Meanwhile, the results of RT-PCR and western blot showed that the expression of FN and Col I decreased in diabetic Pax2-3aFoxO1 mice as compared to diabetic WT mice (Fig. 5E-I). Together, these findings suggest the renoprotective effect of Pax2-3aFoxO1 in the development of renal TIF in diabetic mice.

3.5. Pax2-3aFoxO1 exhibits decreased tubular apoptosis in diabetic mice

Apoptosis of renal tubular epithelial cells is a key feature of the pathogenesis of renal TIF in diabetic mice [27]. To determine whether kidney-specific Pax2-3aFoxO1 was sufficient to reverse the increased tubular apoptosis in diabetic mice, we utilized TUNEL staining and observed a reduction in TUNEL-positive tubular epithelial cells in diabetic Pax2-3aFoxO1 mice compared with diabetic WT mice (Fig. 6A-B). Interestingly, the protein expression of Bax was suppressed in diabetic Pax2-3aFoxO1 mice, but Bcl2 increased as compared to diabetic WT mice (Fig. 6C-E). These results

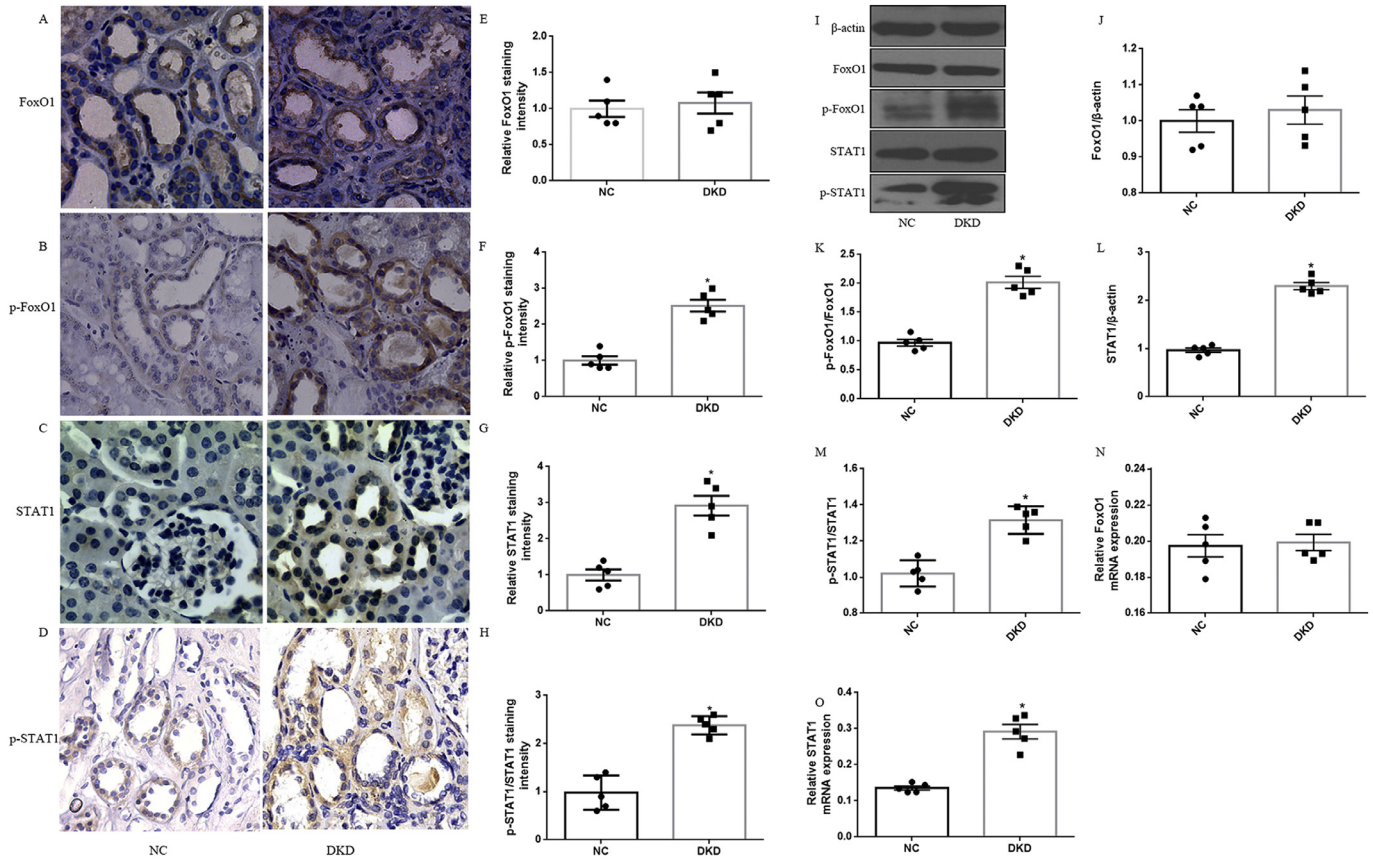

Fig. 1. Human diabetic kidneys show increased expression of p-FoxO1, p-STAT1 and STAT1. (A-D) Representative images of IHC staining for FoxO1, p-FoxO1, STAT1 and p-STAT1 in kidney tissues distant from kidney tumor (NC, $n = 5$) and DKD patients (n = 5). (magnification, 100×). (E-H) Quantification of immunohistochemical staining for FoxO1, p-FoxO1, STAT1 and p-STAT1. (I) Representative western blots for FoxO1, p-FoxO1, STAT1 and p-STAT1 expression in NC group and DKD patients. β-actin was used as a loading control. (J-M) Densitometry of FoxO1, p-FoxO1, STAT1 and p-STAT1 was analyzed. (N–O) RT- PCR analysis for FoxO1 and STAT1 mRNA expression in DKD patients and NC group. Results were normalized with GAPDH levels. The results are expressed as the mean ± SEM, n = 5 kidneys per group, $^{*}P < .05$, P values were determined by unpaired t-test.

supported a key role of Pax2-3aFoxO1 in protecting from tubular apoptosis in diabetic mice.

3.6. 3aFoxO1-KI inhibits EMT in HK-2 cells under HG condition

HG had no effect on FoxO1 gene expression in HK-2 cells, however protein level of p-FoxO1 was significantly elevated (Fig. 7A-C). In order to further explore the mechanism by which FoxO1 regulate EMT, HK-2 cells with 3aFoxO1-KI and FoxO1-KD were constructed via CRISPR/Cas9 genome editing as previously reported (Supplementary Figs. 3 and 4). Efficiency and specificity of 3aFoxO1-KI and FoxO1-KD in cultured HK-2 cells was shown in Supplementary Fig. 5 (3aFoxO1-KI resulted in a 1.9-fold increase, but FoxO1-KD lead about 70% reduction in FoxO1 expression as indicated by RT-PCR, western blot and immunofluorescence staining). The results showed that the expression of α-SMA was up-regulated in HG-induced HK-2 cells, whereas decreased in HK-2 cells with 3aFoxO1-KI (Fig. 7D, F, H). Furthermore, HG-treated HK-2 cells with 3aFoxO1-KI exhibited a significant increase in E-cadherin relative to HG-stimulated HK-2 cells (Fig. 7D, E, G). However, FoxO1-KD aggravated the expression of α-SMA, reduced E-cadherin level (Fig. 7D-H). Collectively, these findings suggest that FoxO1 is critical to preventing EMT under HG conditions.

HG had no effect on FoxO1 gene expression in HK-2 cells, however protein level of p-FoxO1 was significantly elevated (Fig. 7A-C). In order to further explore the mechanism by which FoxO1 regulate EMT, HK-2 cells with 3aFoxO1-KI and FoxO1-KD were constructed via CRISPR/Cas9 genome editing as previously reported (Supplementary Figs. 3 and 4). Efficiency and specificity of 3aFoxO1-KI and FoxO1-KD in cultured HK-2 cells was shown in Supplementary Fig. 5 (3aFoxO1-KI resulted in a 1.9-fold increase, but FoxO1-KD lead about 70% reduction in FoxO1 expression as indicated by RT-PCR, western blot and immunofluorescence staining). The results showed that the expression of α-SMA was up-regulated in HG-induced HK-2 cells, whereas decreased in HK-2 cells with 3aFoxO1-KI (Fig. 7D, F, H). Furthermore, HG-treated HK-2 cells with 3aFoxO1-KI exhibited a significant increase in E-cadherin relative to HG-stimulated HK-2 cells (Fig. 7D, E, G). However, FoxO1-KD aggravated the expression of α-SMA, reduced E-cadherin level (Fig. 7D-H). Collectively, these findings suggest that FoxO1 is critical to preventing EMT under HG conditions.

3.7. 3aFoxO1-KI prevented HG -induced apoptosis in HK-2 cells

HG-treated HK-2 cells with 3aFoxO1-KI exhibited a significant increase in Bcl2 and a reduction in Bax expression as compared to HG-treated WT HK-2 cells or HK-2 cells with FoxO1-KD (Fig. 8A-C). In addition, we also validated these findings by staining for annexin V and propidium iodide by flow cytometry, which showed that 3aFoxO1-KI inhibited apoptosis, whereas FoxO1-KD further enhanced apoptosis in HK-2 cells under HG condition (Fig. 8D-J).

3.8. Elevated STAT1 and TGF-β1 in HK-2 cells and mice under diabetic condition

As results showed that the deactivation of FoxO1 and activation of STAT1 in human kidney induced by diabetes, we hypothe-

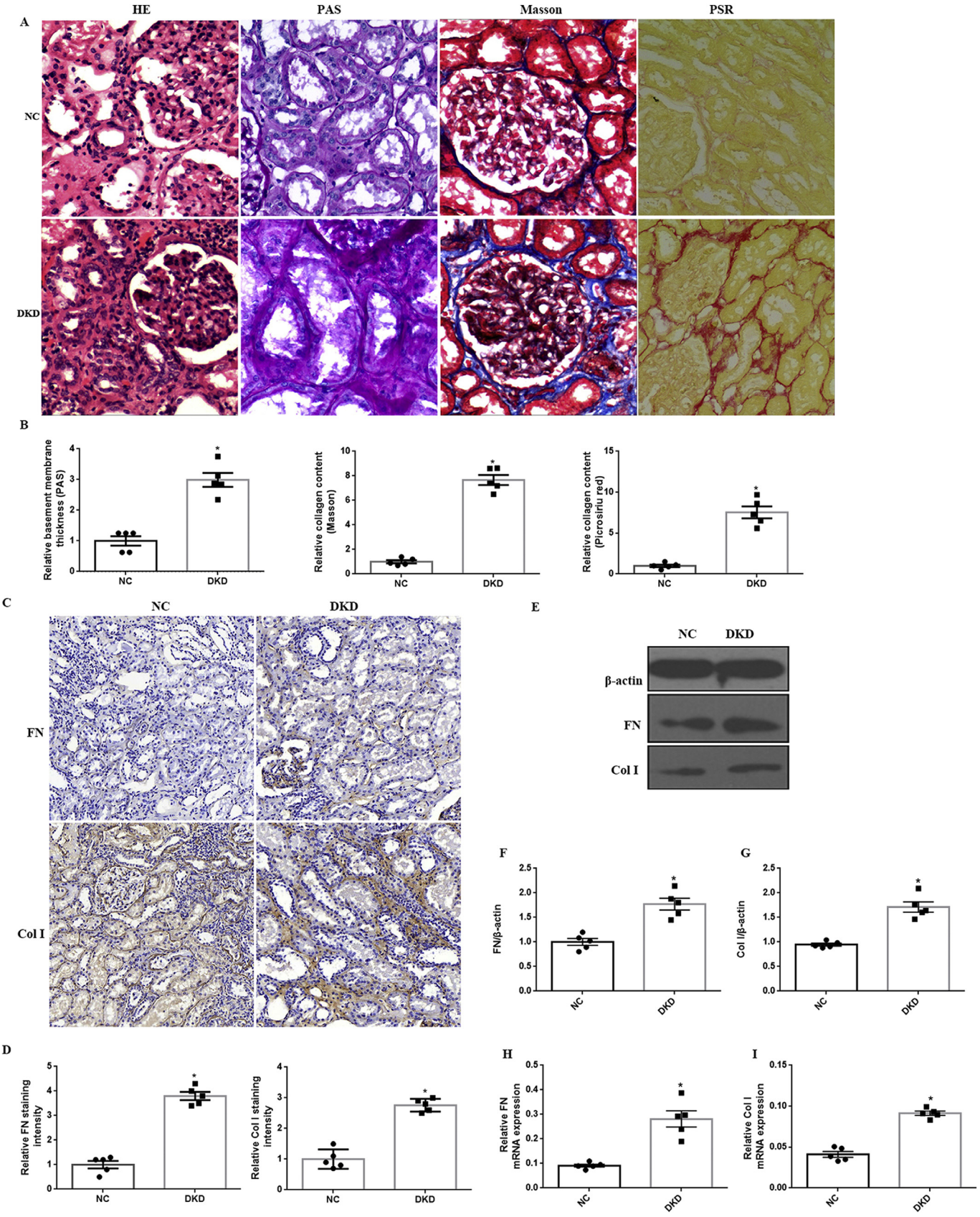

Fig. 2. Histological analysis of kidney injury in DKD patients. (A) Representative images of HE, PAS, Masson and PSR staining (magnification, 100×). (B) Quantification of PAS, Masson and PSR staining. (C) Representative immunohistochemical staining (IHC) for FN and Col I (magnification, 100×). (D) Quantification of IHC staining for FN and Col I. (E) Representative western blot of FN and Col I. (F-G) Densitometry of FN and Col I was analyzed. (H–I) The mRNA levels of FN and Col I were assessed by RT-PCR. The results are expressed as the mean ± SEM, n = 5 kidneys per group, $^{*}P < .05$, *P* values were determined by unpaired *t*-test.

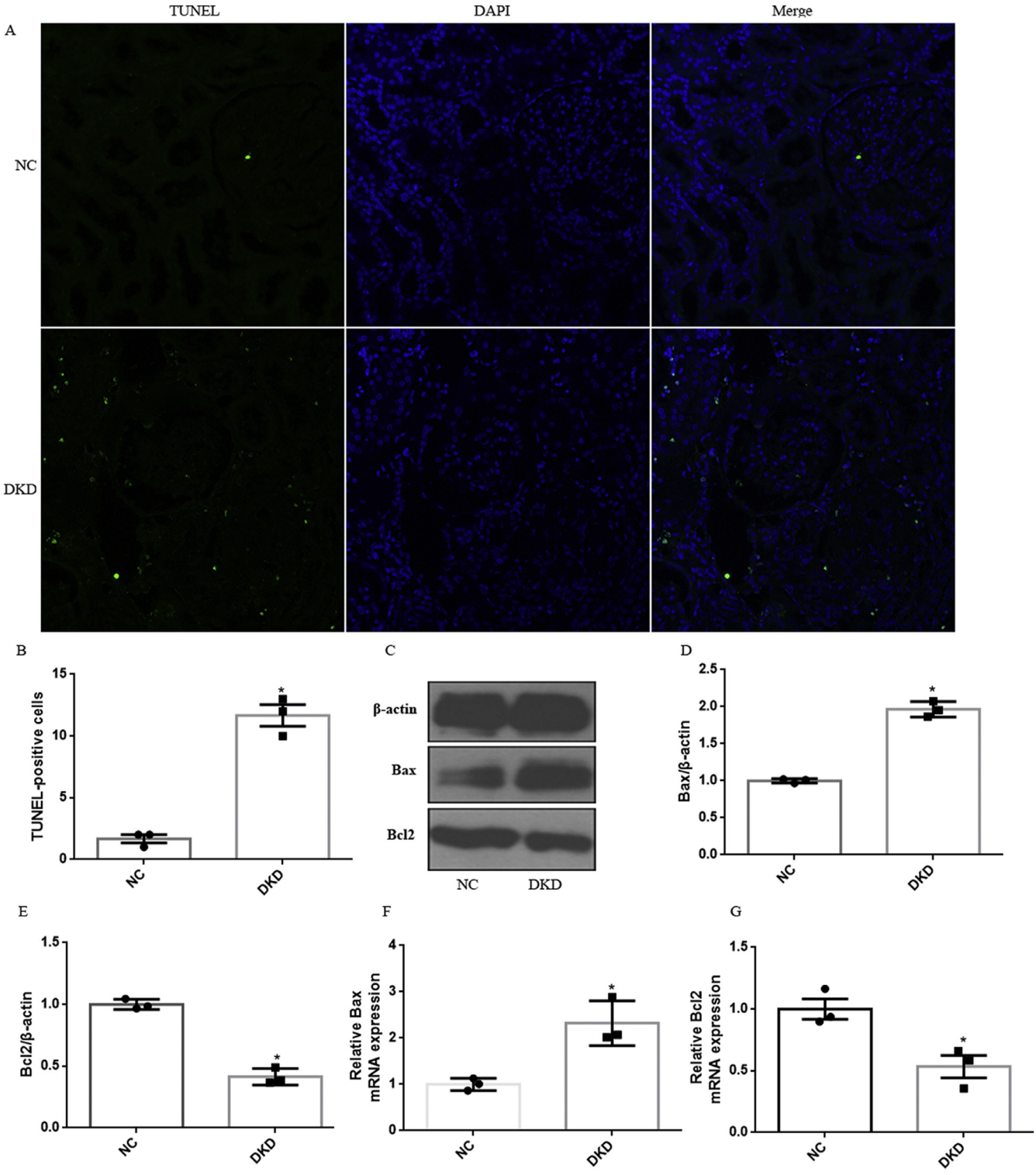

Fig. 3. Diabetic-induced apoptosis in tubular cells in human kidney. (A) Apoptosis was assessed by TUNEL analysis. (B) Results of TUNEL analysis were quantified. (C) Representative western blot of Bax and Bcl-2 in human diabetic kidneys. β-Actin was used as internal control. (D-E) Quantitative analysis of the densitometry of Bax and Bcl-2. (F-G) The mRNA levels of Bax and Bcl-2 were assessed by RT-PCR. All experiments were performed in triplicate. Data were shown as the mean ± SEM, $n = 3$. $^*P < .05$, P values were determined by unpaired t-test.

sized that diabetic Pax2-3aFoxO1 mice would be resistant to renal TIF and tubular apoptosis by STAT1 signaling pathway. As expected, expression level of STAT1 and p-STAT1 was significantly increased in diabetic WT mice, while reversed in diabetic Pax2-3aFoxO1 mice (Fig. 9A-G). Similarly, We observed that HG conditions resulted in increased p-FoxO1, STAT1 and p-STAT1 level in HK-2 cells in dose-dependent manner compared with NG (Supplemental Fig. 6). In addition, the mRNA and protein abundances of STAT1, p-STAT1 and TGFβ1 under HG condition (25 mM) were significantly abrogated by 3aFoxO1-KI, however, aggravated in HK-2 cells with FoxO1-KD (Fig. 9H-L). Meanwhile, we found that knockdown of STAT1 with STAT1 siRNA prevented the increase of STAT1, p-STAT1 and TGF-β1

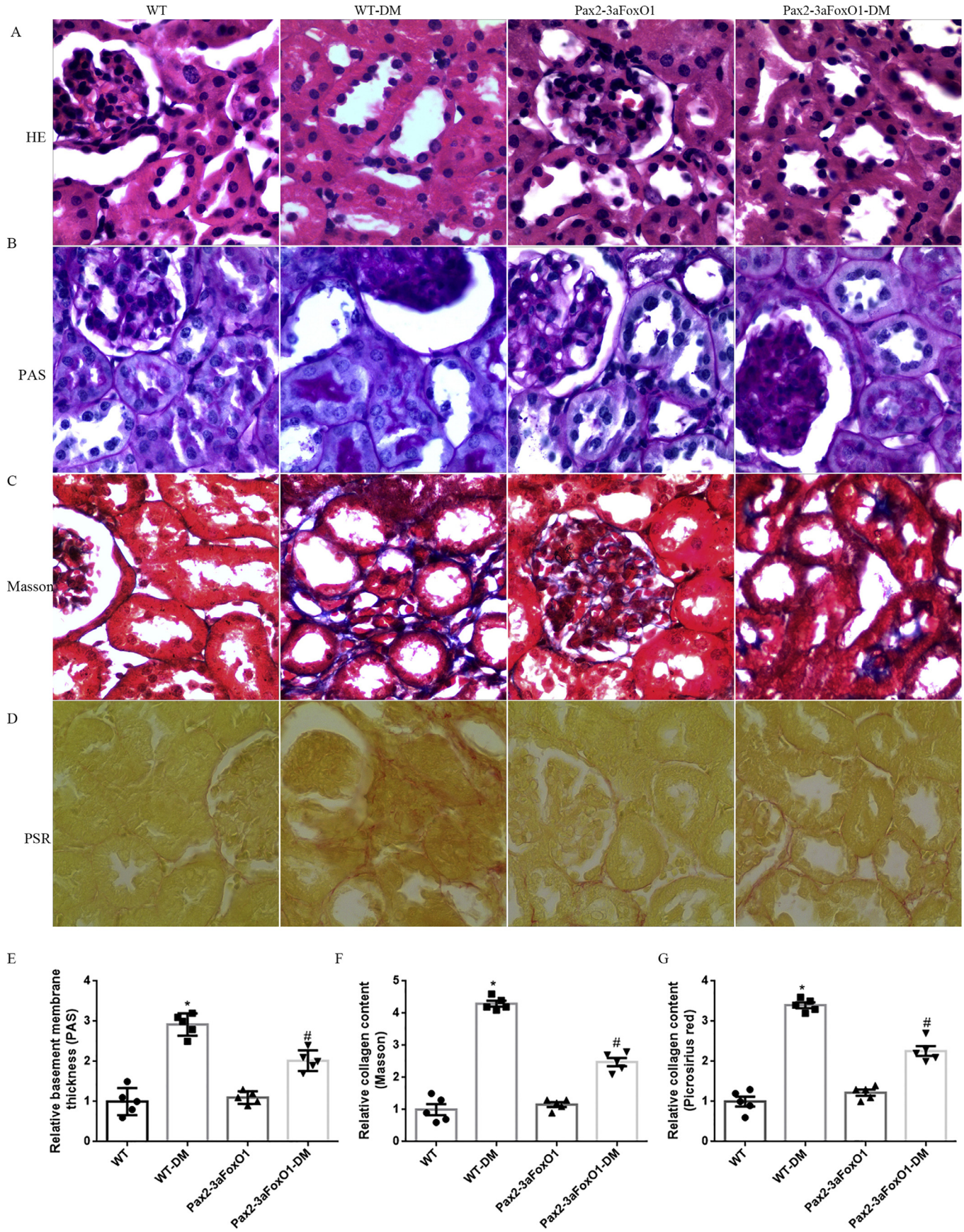

Fig. 4. Kidney-specific Pax2-3aFoxO1 overexpression mice ameliorated renal TIF induced by diabetes in vivo. (A-D) Representative images of HE, PAS, Masson and PSR stainings in mice (magnification, 200×). (E-G) Quantitative analysis of PAS, Masson and PSR stainings. All experiments were performed in triplicate, n = 5 mice per group. Data were shown as the mean ± SEM, $^{*}P < .05$ vs. the WT mice; $\#P < .05$ vs. the WT-DM mice. *P* values were determined by one-way ANOVA analysis.

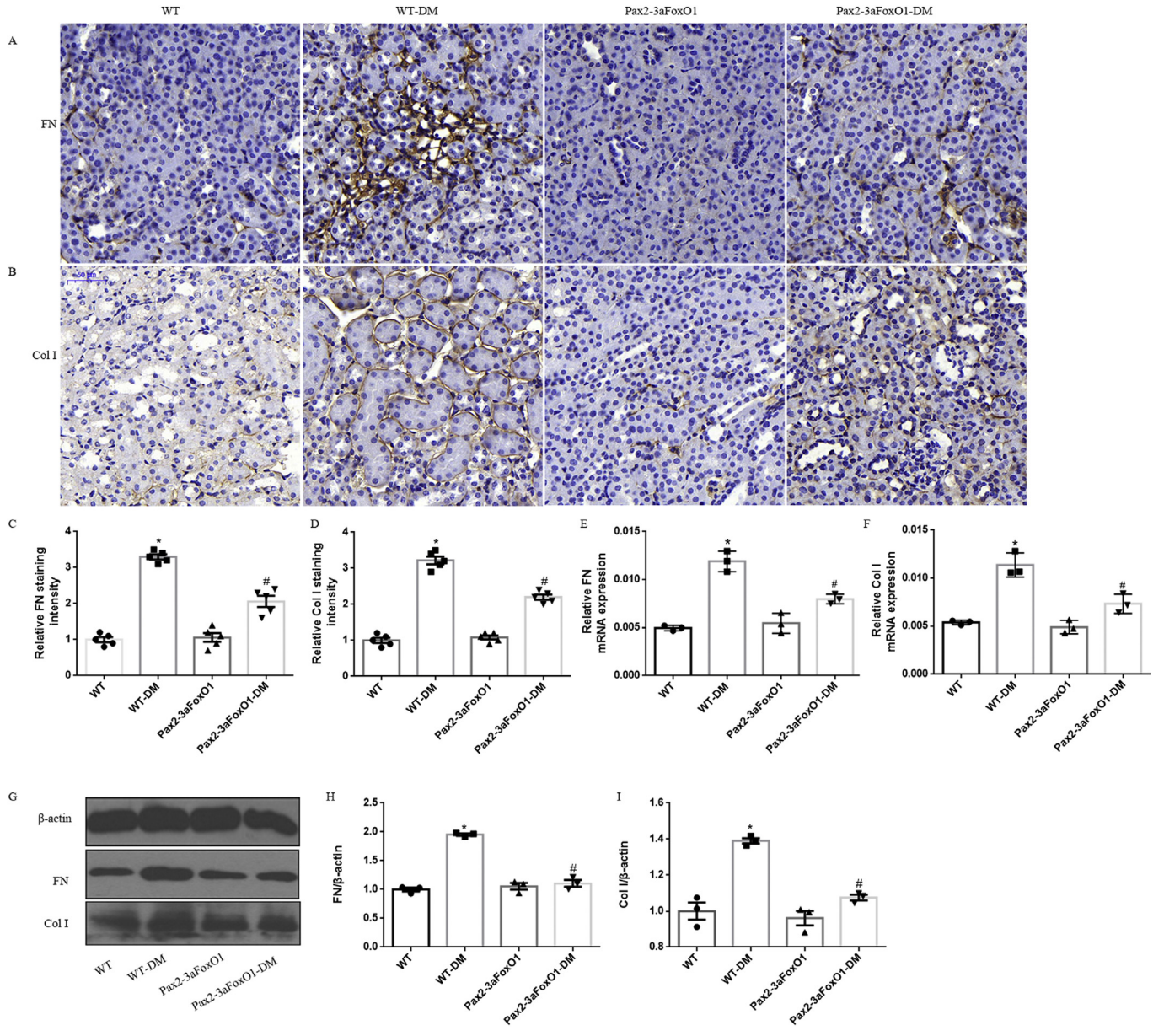

Fig. 5. Diabetic kidney-specific Pax2-3aFoxO1 overexpression mice ameliorated the expression of FN and Col I. (A-B) Representative images for FN and Col I production assessed by IHC analyses in mice. Original magnification, 200×. (C-D) Quantification of IHC staining for FN and Col I in mice. (E-F) The mRNA levels of FN and Col I were assessed by RT-PCR. (G) Representative western blot of FN and Col I. (H-I) Quantitative analysis of the densitometry of FN and Col I . All experiments were performed in triplicate. Data were shown as the mean ± SEM, n = 5, $^{*}P < .05$ vs. the WT mice; $\#P < .05$ vs. the WT-DM mice. *P* values were determined by one-way ANOVA analysis.

in HK-2 cells with FoxO1-KD (Fig. 9H-L). Increased STAT1 and TGF-β1 expression is known to be largely responsible for renal fibrosis in DKD [28,29], but the specific mechanisms are not entirely clear.

As results showed that the deactivation of FoxO1 and activation of STAT1 in human kidney induced by diabetes, we hypothesized that diabetic Pax2-3aFoxO1 mice would be resistant to renal TIF and tubular apoptosis by STAT1 signaling pathway. As expected, expression level of STAT1 and p-STAT1 was significantly increased in diabetic WT mice, while reversed in diabetic Pax2-3aFoxO1 mice (Fig. 9A-G). Similarly, We observed that HG conditions resulted in increased p-FoxO1, STAT1 and p-STAT1 level in HK-2 cells in dose-dependent manner compared with NG (Supplemental Fig. 6). In addition, the mRNA and protein abundances of STAT1, p-STAT1 and TGFβ1 under HG condition (25 mM) were significantly abrogated by 3aFoxO1-KI, however, aggravated in HK-2 cells with FoxO1-KD (Fig. 9H-L). Meanwhile, we found that knockdown of STAT1 with STAT1 siRNA prevented the increase of STAT1, p-STAT1 and TGF-β1 in HK-2 cells with FoxO1-KD (Fig. 9H-L). Increased STAT1 and TGF-β1 expression is known to be largely responsible for renal fibrosis in DKD [28,29], but the specific mechanisms are not entirely clear.

3.9. FoxO1 binds to the promoter of STAT1 in HK-2 cells

To explore how FoxO1 regulates STAT1 expression in tubular epithelial cells, we performed ChIP assays with FoxO1 antibody and tested whether FoxO1 associated with the putative FoxO1-binding sites in the promoter region of *STAT1* in HK-2 cells. The result showed that the abundance of *STAT1* promoter bound to FoxO1 was less in FoxO1-KD HK-2 cells incubated with HG compared with HK-2 cells, whereas 3aFoxO1-KI increased the binding of FoxO1 with the *STAT1* promoter (Fig. 9M-N), and inhibited the activation of STAT1, which indicates a key role of FoxO1/STAT1 signaling pathway in DKD.

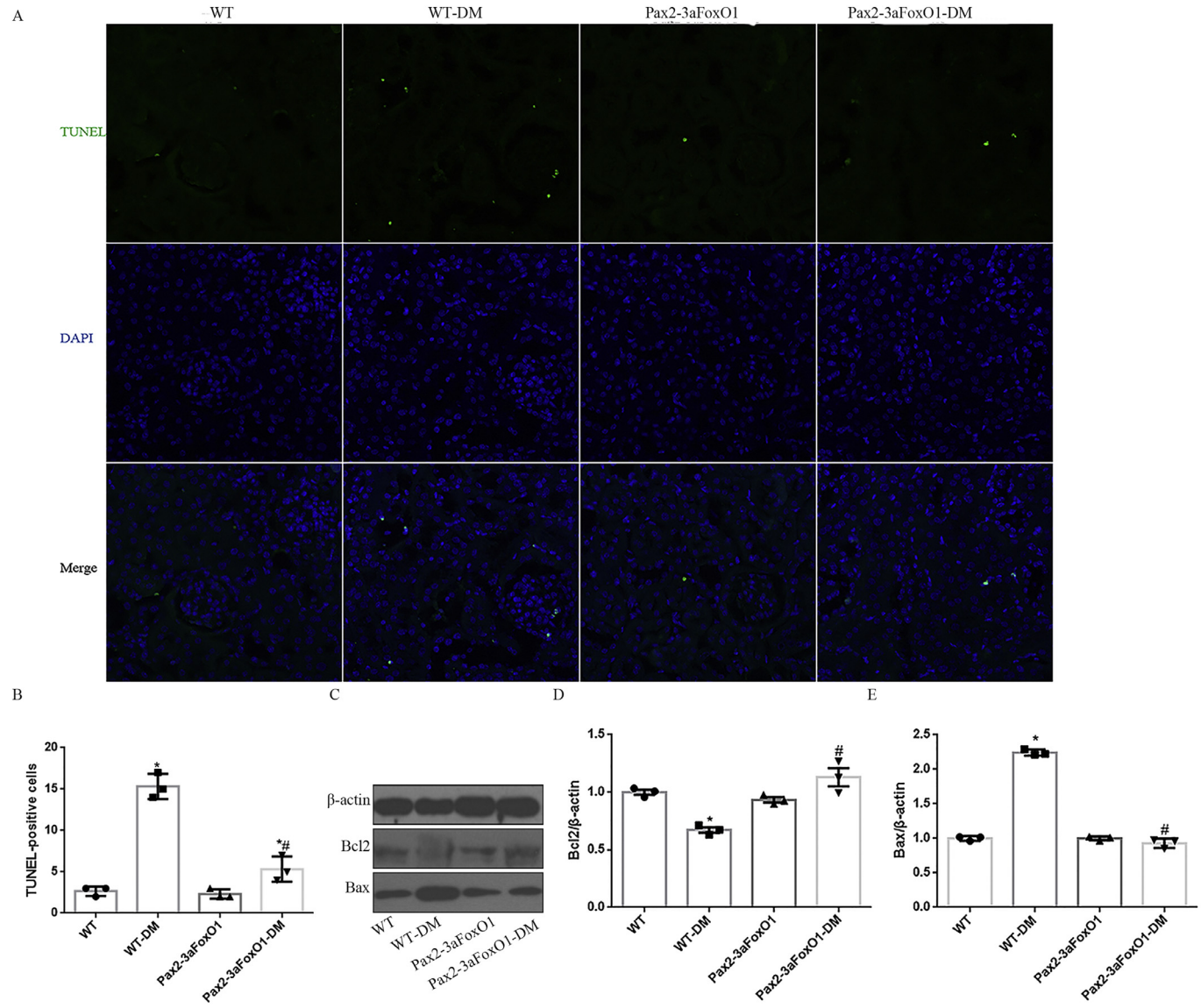

Fig. 6. The effect of FoxO1 on tubular apoptosis in the kidney of diabetic mice. (A) Representative of TUNEL staining showed apoptotic nuclei (green) in diabetic tubules. Original magnification, 200×. (B) Results of TUNEL analysis were quantified. (C) Representative western blot of Bcl2 and Bax in mice kidneys. (D-E) Quantitative analysis of the densitometry of Bcl2 and Bax. Data were shown as the mean ± SEM, n = 5, $^{*}P < .05$ vs. the WT mice; $\#P < .05$ vs. the WT-DM mice. *P* values were determined by one-way ANOVA analysis. (For interpretation of the references to colour in this figure legend, the reader is referred to the web version of this article.)

4. Discussion

The tubulointerstitium comprises 90% of the kidney volume and undergoes major pathological changes in diabetes [30], progressive TIF is the final common pathway in the progression of DKD leading to end-stage renal failure. FoxO1, a transcription factor, is reported to be an upstream regulator of cellular apoptosis and renal fibrosis in multiple cell types, but its function in tubular epithelial cells injuries and renal TIF induced by DKD has not been fully elucidated. Activation of JAK/STAT has been described to play an important mechanism by which hyperglycemia contributes to renal damage [31].

In the current study, we revealed a significant increase of p-FoxO1, p-STAT1 and STAT1 in human renal biopsies with DKD. Moreover, kidney-specific overexpression of Pax2-3aFoxO1 reduced the expression and activation of STAT1 with resultant renal functional impairment, retarding renal TIF and apoptosis in diabetic mice. Meanwhile, We observed that FoxO1-KD in HK-2 cells aggravated the expression of STAT1, leading to activation of EMT and intrinsic apoptotic pathway. Conversely, EMT and apoptosis were significantly attenuated in HK-2 cells with 3aFoxO1-KI under hyperglycemic conditions. These findings provide evidence that FoxO1/STAT1 signaling is required for the development of renal TIF in DKD.

In a small cohort of human kidney biopsies, we observed an increase in collagen content and fibrotic area in patients with DKD as evaluated by Masson and Picrosirius red staining, which is accompanied with the enhanced expression of p-FoxO1, p-STAT1, FN and Col I in tubulointerstitial compartments. Recent accumulating evidence emphasizes the role of FoxO1 in the process of EMT in podocytes in DKD. Several studies have reported that tubular STAT1 might be involved in tubulointerstitial disease in models of DKD. Loredana Fiorentino et al. verified the renoprotective effects of Timp3 by abolishing STAT1 expression in diabetic Timp3(−/−) mice [21]. Moreover, the apoptosis in tubule was up-regulated in DKD patients detected by TUNEL staining. We postulate that FoxO1/STAT1 signaling pathway plays a key role in the develop-

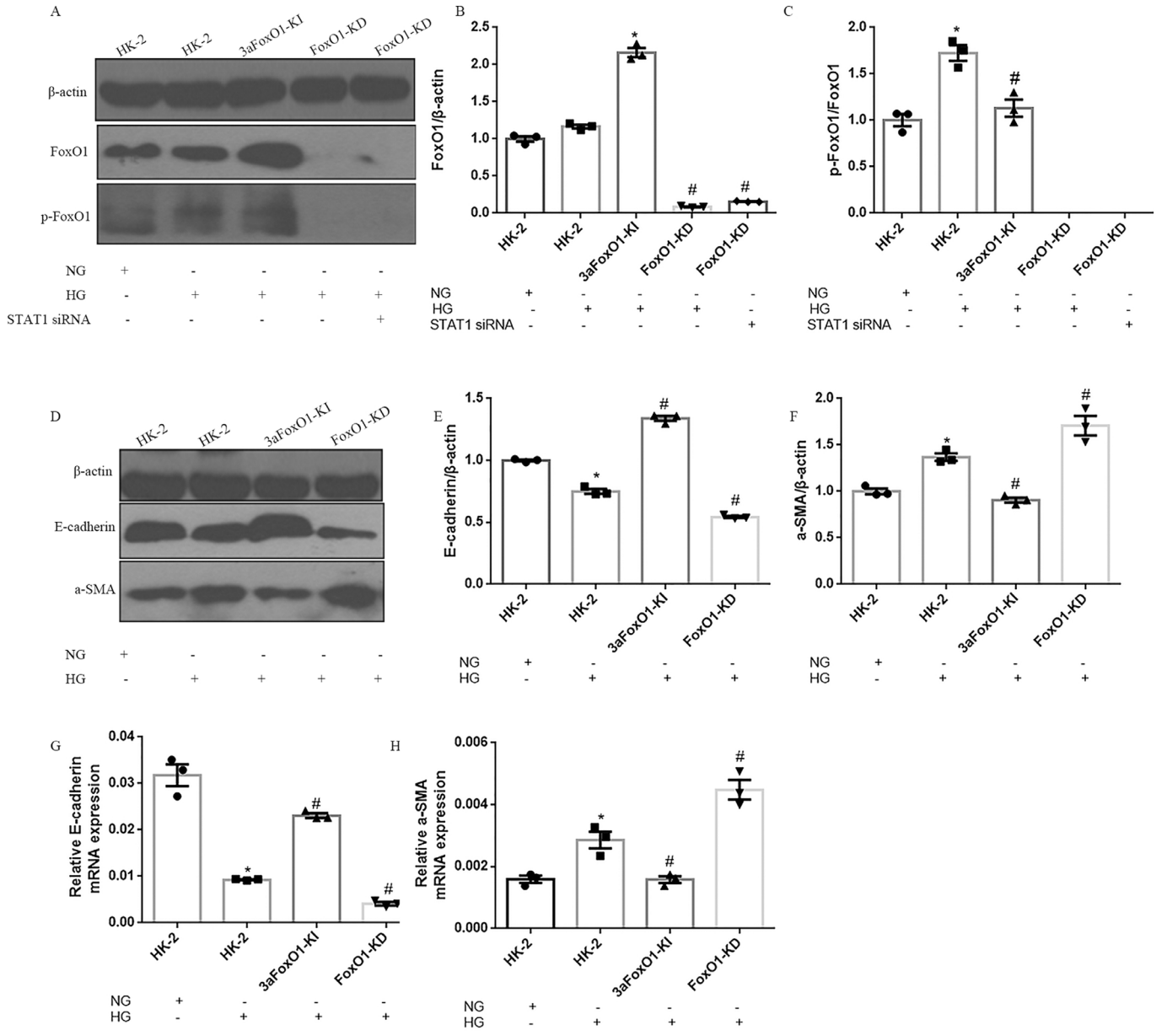

Fig. 7. The effects of FoxO1 on HG induced EMT in HK-2 cells. (A) Representative immunoblotted images of FoxO1 and pFoxO1 in HK-2, 3aFoxO1-KI, and FoxO1-KD cells. (B–C) Quantitative analysis of the densitometry of FoxO1 and p-FoxO1. (D) Representative western blot of E-cadherin and α-SMA. (E-F) Quantitative analysis of the densitometry of E-cadherin and α-SMA. (G–H) RT-PCR analysis of E-cadherin and α-SMA genes expression. Data were shown as the mean ± SEM, $^{*}P < .05$ vs. HK-2 cells incubated with NG; $\#P < .05$ vs. HK-2 cells incubated with HG. *P* values were determined by one-way ANOVA analysis.

ment of DKD, future studies will also need to explore the specific role of FoxO1 in TIF under diabetic condition.

As previously described, kidney-specific overexpression of Pax2-3aFoxO1 results in reduced kidney injury on the C57BL/6 background, but mechanism of which still remain incompletely understood. Chronic activation of JAK/STAT signaling pathway has been reported contributes to diabetic complications by inducing expression of genes involved in cell proliferation, fibrosis, inflammation, and oxidative stress [32]. In the present study, We showed that kidney-specific overexpression of Pax2-3aFoxO1 in STZ-induced diabetic mice is associated with deactivation of STAT1 and reduced 24-h UTP, Scr, BUN, CrCl and KIM-1. However, there is no change in blood glucose. Another interesting finding in the current study was that diabetic Pax2-3aFoxO1 mice decreased tubular apoptosis compared with diabetic WT mice. Besides, we also observed a marked anti-fibrotic effect of 3aFoxO1. Growing evidence suggests that TIF is a pivotal pathophysiological process in patients with DKD [29], we observed that 3aFoxO1 overexpression protected diabetic mice from the development of renal TIF, with a significant reduction in the expression of Col I and FN, as well as collagen content detected by PSR and Masson staining in vivo. In addition, we postulate that deactivation of FoxO1 might contribute to excess STAT1 production leading to increased expression of Col I and FN and tubular basement membrane thickening in diabetic mice. Previous studies have demonstrated STAT1 plays a critical role in renal fibrosis and cellular apoptosis by modulating downstream signaling pathway. The focus of future studies will involve demonstrating the role of FoxO1/STAT1 in renal fibrosis and tubular apoptosis under HG condition.

As is well known, tubular epithelial cells may be involved in the progression of DKD, EMT plays a significant role in renal TIF [33], which is characterized by a loss of epithelial features and acqui-

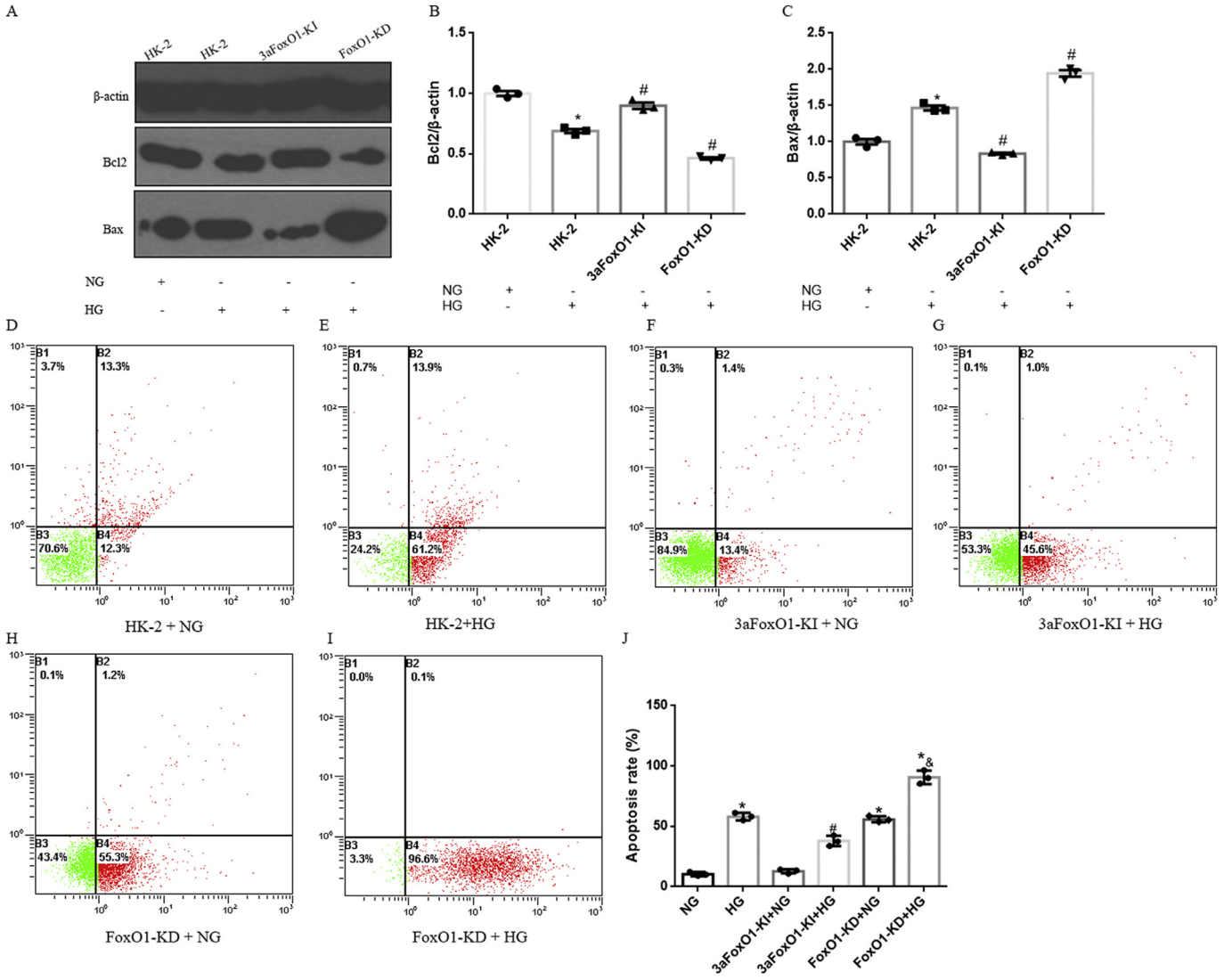

Fig. 8. The effects of FoxO1 on HG induced apoptosis in HK-2 cells. (A) Representative western blots of Bcl2 and Bax in HK-2, 3aFoxO1-KI, and FoxO1-KD cells. (B–C) Quantitative analysis of the densitometry of Bcl2 and Bax. (D–I) HG induced apoptosis in HK-2 was detected by flow cytometry analysis. (J) Results of flow cytometry analysis were quantifiedand. Data were shown as the mean ± SD, $^{*}P < .05$ vs. HK-2 cells incubated with NG; $\#P < .05$ vs. HK-2 cells incubated with HG. $\&P < .05$ vs. FoxO1-KD cells with NG. *P* values were determined by one-way ANOVA analysis.

sition of mesenchymal markers [34], leading to structural damage and dysfunction of the kidneys [35]. Thus, identifying the mechanisms of EMT activation could be meaningful in the pathogenesis and progression of DKD. However, the EMT-regulating signal transduction pathways are complicated and have not yet been fully elucidated. In line herewith, our studies in cultured HK-2 cells mimicking hyperglycaemic and diabetes conditions demonstrated that 3aFoxO1-KI inhibited the process of EMT. STAT1 is known as the major inducer that initiates and completes the EMT process, a crucial downstream pathway associated with renal fibrosis [36]. Here, we observed that HK-2 cells with 3aFoxO1-KI dramatically downregulated STAT1 and p-STAT1 expression, but FoxO1-KD had the opposite effect. These findings provide strong evidence that STAT1 signaling is involved in FoxO1-mediated reduction of EMT and renal TIF. Furthermore, we found that silencing of STAT1 by STAT1 siRNA blocked FoxO1 KD-induced EMT in HG condition. These results further supports the hypothesis that STAT1 is an essential protein participating in EMT induced by HG and a crucial effector downstream of FoxO1. Our findings are consistent with the notion that a significant increase in STAT1 contributes to renal fibrosis and the production of profibrotic cytokine through TGF-β1 [37], as well as with the critical role of STAT1 in the progression of liver fibrosis and the fact that suppression of STAT1promotes the reversion of liver fibrosis and recovery [38].

Renal tubular epithelial cell apoptosis, contributes to the development of DKD, is an important feature of TIF that reduces the normal function of renal tubules, induces renal tubular atrophy, and promotes TIF progression [39], but the mechanisms that lead to diabetes-induced cell death are not fully understood. In this study, we observed that 3aFoxO1-KI inhibited Bax expression and apoptosis, but maintained Bcl2 expression in HK-2 cells. Moreover, silencing of STAT1 by STAT1 siRNA blocked FoxO1 KD-regulated apoptosis in HG condition. In addition, diabetic Pax2-3aFoxO1 mice also significantly decreased tubular damage and apoptotic tubular epithelial cells compared with diabetic WT mice. Notably, it has been reported that knockdown of STAT1 suppressed cell death, which is in good agreement with our findings, highlighting the importance of the pro-death role of STAT1 as a new approach to treat kidney fibrosis [40]. Oxidative stress resulting from excessive production of reactive oxygen species (ROS) or impaired antioxidant defenses is closely related to the development of DKD. It has been reported that hyperglycaemia-induced oxidative stress plays

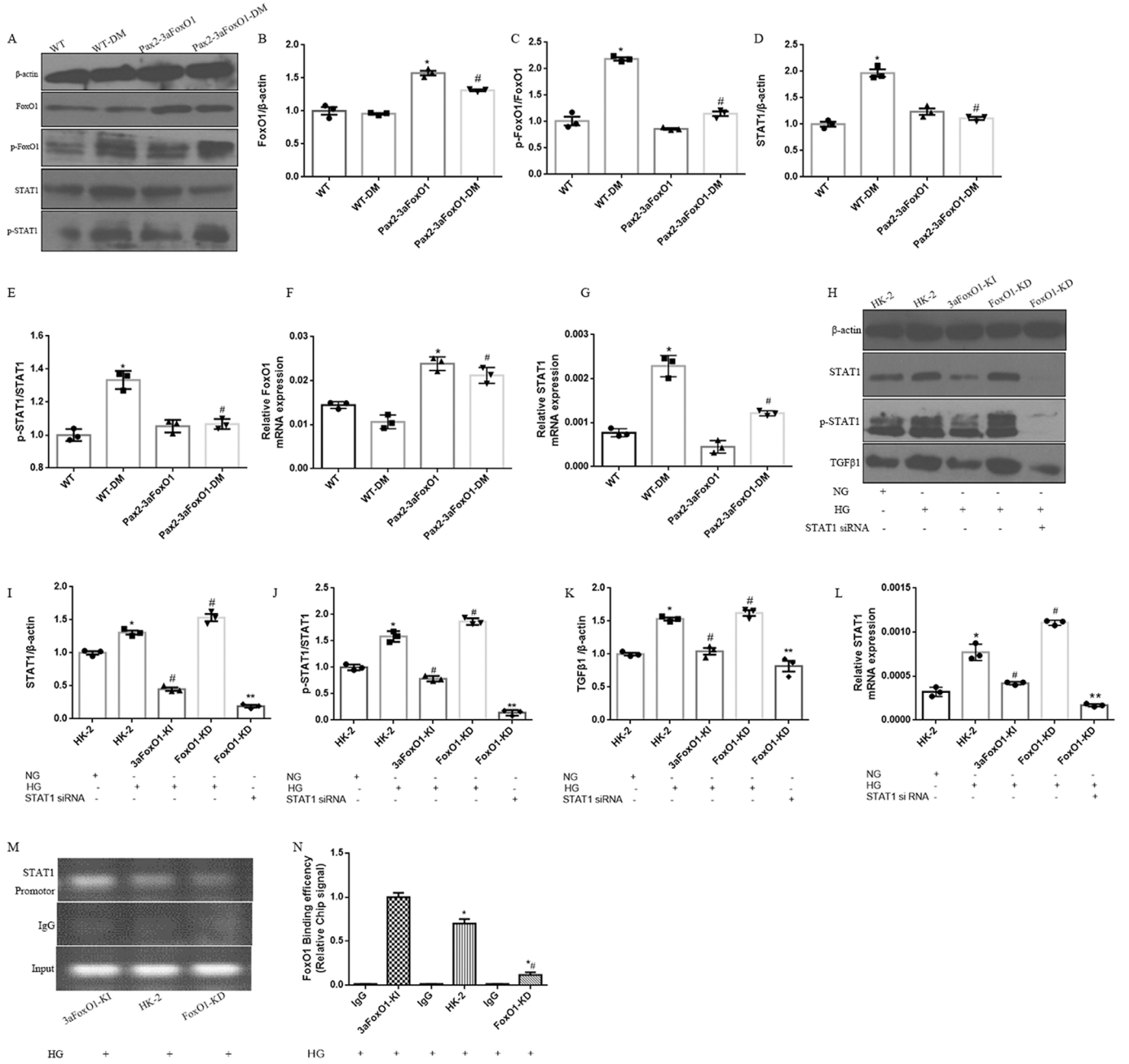

Fig. 9. Effects of FoxO1 on HG-induced activation of STAT1 signaling pathway. (A) Representative western blot of FoxO1, p-FoxO1, STAT1 and p-STAT1 in diabetic mice kidneys. (B–E) Quantitative analysis of the densitometry of FoxO1, p-FoxO1, STAT1 and p-STAT1. (F–G) The mRNA levels of FoxO1 and STAT1 were assessed by RT-PCR. Data were shown as the mean ± SEM, $^{*}P < .05$ vs. the WT mice; $\#P < .05$ vs. the WT-DM mice. *P* values were determined by one-way ANOVA analysis. (H) Representative western blot of STAT1, p-STAT1 and TGFβ1 in HK-2 cells. (I–K) Quantitative analysis of the densitometry of STAT1, p-STAT1 and TGFβ1. (L) The mRNA level of STAT1 was assessed by RT-PCR. Data were shown as the mean ± SEM, $^{*}P < .05$ vs. HK-2 cells incubated with NG; $\#P < .05$ vs.HK-2 cells incubated with HG; $^{**}P < .05$ vs. FoxO1-KD incubated with HG. *P* values were determined by one-way ANOVA analysis. (M) Nuclear extracts in HK-2, 3aFoxO1-KI and FoxO1-KD cells were immunoprecipitated with anti-FoxO1 antibody or IgG. (N) Quantitative analysis of the results of ChIP assay. IgG from rabbit served as a control. Data were shown as the mean ± SD, $^{*}P < .05$ vs. 3aFxoO1-KI cells incubated with HG; $\#P < .05$ vs. HK-2 cells incubated with HG. *P* values were determined by one-way ANOVA analysis.

an important role in the progression and severity of DKD. Previous studies have confirmed that hyperglycemia could contribute to the development of DKD through JAK/STATs signaling pathway. It is possible that 3aFoxO1 overexpression may inhibit tubular apoptosis and TIF by suppressing oxidative stress via JAK-STAT signaling cascade, but the mechanism remains unresolved. The focus of future studies will involve demonstrating the antioxidant role of FoxO1 in the tubular epithelial cells.

Meanwhile, ChIP assay demonstrated that FoxO1 can directly bind with the promoter of *STAT1*, and down-regulated the level of STAT1 in FoxO1-KI HK-2 cells. However, FoxO1-KD reduced FoxO1-STAT1 binding activity, increased STAT1 expression in HK-2 cells. Moreover, previous studies have provided evidence that STAT1 had a negative effect on FoxO1 transcription [41] and that abolishing STAT1 expression rescues the FoxO1 level [21] . These studies collectively established that FoxO1 and STAT1 may form a negative feedback loop and maintain anti-fibrosis homeostasis in renal tubular cells. However, the precise correlation between FoxO1 and STAT1 in DKD needs to be further confirmed by a dual-luciferase reporter assay in future studies.

In conclusion, these data suggest that kidney-specific Pax2-3aFoxo1 overexpression ameliorates renal TIF and tubular apoptosis through the attenuation of STAT1 signaling pathway under diabetic conditions. Indeed, these data imply the FoxO1/STAT1 axis as an effective and safe target, at least in part, in the pathogenesis of TIF and apoptosis in DKD.

Funding sources

This study was supported by grants from the National Natural Science Foundation of China (grant numbers: 81570746 and 81770812). G.Q is the guarantor of this work, had full access to all the data, and take full responsibility for the integrity of data and the accuracy of data analysis.

Author contributions

F.H. designed, performed and analyzed experiments. F.G. and Q.W contributed to revise the manuscript. Y.Z. contributed to produce figures, and Y.L. contributed to preparation of human kidney specimens, Y.H. contributed to immunofluorescence experiments, L.J. and Y.S. contributed to cell culture, T.A contributed to tissue collection from mouse. G.Q. supervises the experiment and takes responsibility for the integrity of the data and the accuracy of the data analysis. All authors commented on the manuscript.

Declaration of Competing Interest

The authors declare no competing financial interests.

Appendix A. Supplementary data

Supplementary data to this article can be found online at https://doi.org/10.1016/j.ebiom.2019.09.002.

References

[1] Cefalu WT, Buse JB, Tuomilehto J, Fleming GA, Ferrannini E, Gerstein HC, et al. Update and next steps for real-world translation of interventions for type 2 diabetes prevention: reflections from a diabetes care editors' expert forum. Diabetes Care 2016;39(7):1186–201.
[2] Nauta FL, Boertien WE, Bakker SJ, van Goor H, van Oeveren W, de Jong PE, et al. Glomerular and tubular damage markers are elevated in patients with diabetes. Diabetes Care 2011;34(4):975–81.
[3] Gilbert RE, Cooper ME. The tubulointerstitium in progressive diabetic kidney disease: more than an aftermath of glomerular injury? Kidney Int. 1999;56(5):1627–37.
[4] Anorga S, Overstreet JM, Falke LL, Tang J, Goldschmeding RG, Higgins PJ, et al. Deregulation of Hippo-TAZ pathway during renal injury confers a fibrotic maladaptive phenotype. FASEB J. 2018;32(5):2644–57.
[5] Liu Y. Epithelial to mesenchymal transition in renal fibrogenesis: pathologic significance, molecular mechanism, and therapeutic intervention. J Am Soc Nephrol 2004;15(1):1–12.
[6] Ruggenenti P, Cravedi P, Remuzzi G. The RAAS in the pathogenesis and treatment of diabetic nephropathy. Nat Rev Nephrol 2010;6(6):319–30.
[7] Calnan DR, Brunet A. The FoxO code. Oncogene 2008;27(16):2276–88.
[8] Maiese K, Hou J, Chong ZZ, Shang YC. A fork in the path: developing therapeutic inroads with FoxO proteins. Oxidative Med Cell Longev 2009;2(3):119–29.
[9] Guo F, Wang Q, Zhou Y, Wu L, Ma X, Liu F, et al. Lentiviral vector-mediated FoxO1 overexpression inhibits extracellular matrix protein secretion under high glucose conditions in mesangial cells. J. Cell. Biochem. 2016;117(1):74–83.
[10] Qin G, Zhou Y, Guo F, Ren L, Wu L, Zhang Y, et al. Overexpression of the FoxO1 ameliorates mesangial cell dysfunction in male diabetic rats. Mol. Endocrinol. 2015;29(7):1080–91.
[11] Guo F, Zhang Y, Wang Q, Ren L, Zhou Y, Ma X, et al. Effects of FoxO1 on podocyte injury in diabetic rats. Biochem. Biophys. Res. Commun. 2015;466(2):260–6.
[12] Stark GR, Darnell JJ. The JAK-STAT pathway at twenty. Immunity 2012;36(4):503–14.
[13] Begitt A, Droescher M, Meyer T, Schmid CD, Baker M, Antunes F, et al. STAT1-cooperative DNA binding distinguishes type 1 from type 2 interferon signaling. Nat. Immunol. 2014;15(2):168–76.
[14] Bowman T, Garcia R, Turkson J, Jove R. STATs in oncogenesis. Oncogene 2000;19(21):2474–88.
[15] CV R, H N, GR S, Kishore MC. Complex roles of Stat1 in regulating gene expression. Oncogene 2000;19(21):2619–27.
[16] Stark GR, Darnell JJ. The JAK-STAT pathway at twenty. Immunity 2012;36(4):503–14.
[17] Zhao SQ, Shen ZC, Gao BF, Han P. microRNA-206 overexpression inhibits epithelial-mesenchymal transition and glomerulosclerosis in rats with chronic kidney disease by inhibiting JAK/STAT signaling pathway. J. Cell. Biochem. 2019;120(9):14604–17.
[18] Huang JS, Chuang LY, Guh JY, Chen CJ, Yang YL, Chiang TA, et al. Effect of nitric oxide-cGMP-dependent protein kinase activation on advanced glycation end-product-induced proliferation in renal fibroblasts. J Am Soc Nephrol 2005;16(8):2318–29.
[19] Nakajima H, Takenaka M, Kaimori JY, Hamano T, Iwatani H, Sugaya T, et al. Activation of the signal transducer and activator of transcription signaling pathway in renal proximal tubular cells by albumin. J Am Soc Nephrol 2004;15(2):276–85.
[20] Nightingale J, Patel S, Suzuki N, Buxton R, Takagi KI, Suzuki J, et al. Oncostatin M, a cytokine released by activated mononuclear cells, induces epithelial cell-myofibroblast transdifferentiation via Jak/Stat pathway activation. J Am Soc Nephrol 2004;15(1):21–32.
[21] Fiorentino L, Cavalera M, Menini S, Marchetti V, Mavilio M, Fabrizi M, et al. Loss of TIMP3 underlies diabetic nephropathy via FoxO1/STAT1 interplay. EMBO Mol Med 2013;5(3):441–55.
[22] Wang H, Zhang Y, Xia F, Zhang W, Chen P, Yang G. Protective effect of silencing Stat1 on high glucose-induced podocytes injury via Forkhead transcription factor O1-regulated the oxidative stress response. BMC Mol Cell Biol 2019;20(1):27.
[23] Huang F, Wang Q, Ma X, Wu L, Guo F, Qin G. Valsartan inhibits amylin-induced podocyte damage. Microvasc. Res. 2016;106:101–9.
[24] Singh S, Manson SR, Lee H, Kim Y, Liu T, Guo Q, et al. Tubular overexpression of Angiopoietin-1 attenuates renal fibrosis. PLoS One 2016;11(7):e0158908.
[25] Li W, Du M, Wang Q, Ma X, Wu L, Guo F, et al. FoxO1 promotes mitophagy in the podocytes of diabetic male mice via the PINK1/parkin pathway. Endocrinology 2017;158(7):2155–67.
[26] Ji L, Wang Q, Huang F, An T, Guo F, Zhao Y, et al. FOXO1 overexpression attenuates tubulointerstitial fibrosis and apoptosis in diabetic kidneys by ameliorating oxidative injury via TXNIP-TRX. Oxidative Med. Cell. Longev. 2019;2019:3286928.
[27] Docherty NG, O'Sullivan OE, Healy DA, Fitzpatrick JM, Watson RW. Evidence that inhibition of tubular cell apoptosis protects against renal damage and development of fibrosis following ureteric obstruction. Am J Physiol Renal Physiol 2006;290(1):F4–13.
[28] Fernandez-Fernandez B, Ortiz A, Gomez-Guerrero C, Egido J. Therapeutic approaches to diabetic nephropathy—beyond the RAS. Nat. Rev. Nephrol. 2014;10(6):325–46.
[29] Fischer C, Deininger N, Wolf G, Loeffler I. CERA attenuates kidney fibrogenesis in the db/db mouse by influencing the renal myofibroblast generation. J. Clin. Med. 2018;7(2).
[30] EG N. Mechanisms of tubulointerstitial fibrosis. Curr. Opin. Nephrol. Hypertens. 2004;13(3):279–84.
[31] Ortiz-Muñoz G, Lopez-Parra V, Lopez-Franco O, Fernandez-Vizarra P, Mallavia B, Flores C, et al. Suppressors of cytokine signaling abrogate diabetic nephropathy. J Am Soc Nephrol 2010(5):763–72.
[32] Lopez-Sanz L, Bernal S, Recio C, Lazaro I, Oguiza A, Melgar A, et al. SOCS1-targeted therapy ameliorates renal and vascular oxidative stress in diabetes via STAT1 and PI3K inhibition. Lab. Investig. 2018;98(10):1276–90.
[33] Zhao Y, Yin Z, Li H, Fan J, Yang S, Chen C, et al. MiR-30c protects diabetic nephropathy by suppressing epithelial-to-mesenchymal transition in db/db mice. Aging Cell 2017;16(2):387–400.
[34] Liu Y. New insights into epithelial-mesenchymal transition in kidney fibrosis. J Am Soc Nephrol 2010;21(2):212–22.
[35] Rastaldi MP. Epithelial-mesenchymal transition and its implications for the development of renal tubulointerstitial fibrosis. J Nephrol 2006;19(4):407–12.
[36] Kachroo P, Lee MH, Zhang L, Baratelli F, Lee G, Srivastava MK, et al. IL-27 inhibits epithelial-mesenchymal transition and angiogenic factor production in a STAT1-dominant pathway in human non-small cell lung cancer. J. Exp. Clin. Cancer Res. 2013;32:97.
[37] Wang P, Yang J, Tong F, Duan Z, Liu X, Xia L, et al. Anti-double-stranded DNA IgG participates in renal fibrosis through suppressing the suppressor of cytokine signaling 1 signals. Front. Immunol. 2017;8:610.
[38] Zhang H, Chen F, Fan X, Lin C, Hao Y, Wei H, et al. Quantitative proteomic analysis on activated hepatic stellate cells reversion reveal STAT1 as a key regulator between liver fibrosis and recovery. Sci. Rep. 2017;7:44910.
[39] Chen JF, Wu QS, Xie YX, Si BL, Yang PP, Wang WY, et al. TRAP1 ameliorates renal tubulointerstitial fibrosis in mice with unilateral ureteral obstruction by protecting renal tubular epithelial cell mitochondria. FASEB J. 2017;31(10):4503–14.
[40] Wang S, Liu A, Wu G, Ding HF, Huang S, Nahman S, et al. The CPLANE protein Intu protects kidneys from ischemia-reperfusion injury by targeting STAT1 for degradation. Nat. Commun. 2018;9(1):1234.
[41] Luo Y, Lin Y, Han X. Original article. Transcription factors regulate Forkhead box O1 gene promoter activity in pancreatic β-cells. Asian Biomedicine 2011;5(4):433–9.